CrossMark

ORIGINAL ARTICLE

Early imaging findings in germ cell tumors arising from the basal ganglia

So Mi Lee[1,3] · In-One Kim[2] · Young Hun Choi[2] · Jung-Eun Cheon[2] ·
Woo Sun Kim[2] · Hyun-Hae Cho[1,4] · Sun Kyoung You[1,5]

Abstract

Background It is difficult to diagnosis early stage germ cell tumors originating in the basal ganglia, but early recognition is important for better outcome.

Objective To evaluate serial MR images of basal ganglia germ cell tumors, with emphasis on the features of early stage tumors.

Materials and methods We retrospectively reviewed serial MR images of 15 tumors in 14 children and young adults. We categorized MR images of the tumors as follows: type I, ill-defined patchy lesions (<3 cm) without cyst; type II, small mass lesions (<3 cm) with cyst; and type III, large lesions (≥3 cm) with cyst. We also assessed temporal changes of the MR images.

Results On the initial images, 8 of 11 (73%) type I tumors progressed to types II or III, and 3 of 4 (75%) type II tumors progressed to type III. The remaining 4 tumors did not change in type. All type II tumors (5/5, 100%) that changed from type I had a few tiny cysts. Intratumoral hemorrhage was observed even in the type I tumor. Ipsilateral hemiatrophy was observed in most of the tumors (13/15, 87%) on initial MR images. As tumors grew, cystic changes, intratumoral hemorrhage, and ipsilateral hemiatrophy became more apparent.

Conclusion Early stage basal ganglia germ cell tumors appear as ill-defined small patchy hyperintense lesions without cysts on T2-weighted images, are frequently associated with ipsilateral hemiatrophy, and sometimes show microhemorrhage. Tumors develop tiny cysts at a relatively early stage.

Keywords Adolescent · Basal ganglia · Child · Early stage · Germ cell tumor · Magnetic resonance imaging · Serial images

✉ In-One Kim
  kimio@snu.ac.kr

1 Department of Radiology,
   Seoul National University College of Medicine,
   101 Daehak-ro, Jongno-gu Seoul 110-769,
   Republic of Korea

2 Department of Radiology and Institute of Radiation Medicine,
   Seoul National University College of Medicine,
   101 Daehak-ro, Jongno-gu Seoul 110-769,
   Republic of Korea

3 Department of Radiology,
   Kyungpook National University Medical Center,
   807 Hoguk-ro, Buk-gu, Daegu 41404, Republic of Korea

4 Department of Radiology,
   Ewha Woman's University Mokdong Hospital,
   Seoul, South Korea

5 Department of Radiology,
   Chungnam National University Hospital,
   Daejeon, Republic of Korea

Introduction

Intracranial germ cell tumors usually originate in the pineal, suprasellar or other midline region but rarely in the basal ganglia or thalamus [1–3]. Children with early stage germ cell tumors in the basal ganglia frequently present with vague symptoms such as slowly progressive hemiparesis and cognitive decline [4]. Neuroimaging findings are often subtle [5–8], which can delay diagnosis until an advanced disease stage, when classic images show overt large masses with intratumoral hemorrhage and various-size cysts [3, 5, 7–10].

Because germ cell tumors are relatively radiosensitive and potentially curable [1, 2], early recognition is important for better outcome. Therefore, many reports have described early MRI findings of germ cell tumors in the basal ganglia [5–7, 11, 12]. Early stage germ cell tumors usually appear as ill-defined hyperintense lesions on T2-weighted images [6–9, 12–15] and are sometimes unnoticeable, showing only subtle changes during

follow-up that make it difficult to differentiate germ cell tumors from other glial tumors and non-tumorous conditions such as infarction and demyelinating disease [12, 16]. Moreover, unusual images or unfamiliar features of the tumor during disease progression can make it even more difficult to diagnose germ cell tumor. Although ^{11}C-methionin positron emission tomography can be a promising diagnostic modality in the early stages [17, 18], clinical and radiologic suspicion is needed to perform this study. Additionally, this study can be inconclusive in cases of weak uptake [16, 19, 20].

Therefore, diagnosis of early stage basal ganglia germ cell tumors remains challenging and examination of consecutive neuroimaging scans is often necessary. Accordingly, knowledge about sequential imaging findings of a basal ganglia germ cell tumors can aid earlier diagnosis by differentiating germ cell tumors from other diseases [5–7, 9, 11]. This study defines the early MR features of the basal ganglia germ cell tumor from a review of serial MR features in these tumors.

Materials and methods

Patients

Our institutional review board approved this study and waived the requirement for informed consent. From 2000 to 2013, 38 children and young adults were diagnosed with basal ganglia germ cell tumors at our institution. We excluded 24 patients who were diagnosed with germ cell tumor after a single MR examination; all 24 of these patients had an overt mass larger than 3 cm with various-size cysts leading to clear diagnosis within 30 days of the initial MRI. The remaining 14 patients underwent more than two MR examinations before diagnosis and had a delayed diagnosis; delayed diagnosis in these cases was a result of biopsy refusal or unfamiliar MRI presentation. We included these 14 patients in the study. These 14 patients had a total of 15 tumors; 1 had bilateral tumors. The male-to-female ratio was 12:2; mean age was 12.6 years (range 7–19 years). Twelve patients had germinomas confirmed via stereotactic biopsy. The remaining two patients were diagnosed with potential germ cell tumors because of (cerebrospinal fluid reference level: alpha-fetoprotein <1.5 ng/mL; beta-human chorionic gonadotropin <2mIU/ml); beta-human chorionic gonadotropin <2mIU/ml); both had highly elevated beta-human chorionic gonadotropin levels in cerebrospinal fluid (380 mIU/ml and 118 mIU/ml, respectively), and one also had elevated cerebrospinal fluid alpha-fetoprotein levels (221 ng/ml) [21, 22].

MR image analysis

We retrospectively reviewed 48 serial MRI examinations (2–6 per patient; mean 3.4 per patient) in 14 children and young adults; 21 of 48 MRI examinations were performed at another hospital before transfer to our tertiary hospital, so the timing and protocols of the MRI examinations varied. MR images were acquired on a 1.5-T MR unit in 41 examinations, a 3-T unit in 7. The examinations included axial unenhanced T1-weighted (repetition time [TR]/echo time [TE]=450–650/8–25 ms) and T2-weighted (TR/TE=3,000–6,200/80–136 ms) spin-echo images (all patients); fluid-attenuated inversion recovery images (FLAIR) (TR/TE/inversion time [TI]=6,000–9,000/90–120/2, 000–2,500 ms) (43 examinations); axial post-contrast T1-weighted images (40 examinations); and susceptibility-weighted images or T2*-weighted gradient-echo MR images (14 examinations). Other parameters examined: slice thickness=2–5 mm; interslice gap=0–2 mm; acquisition matrix=185–450×160–371; and field of view (FOV)=16–24×21–24 cm.

After reviewing all serial MR images we classified the basal ganglia germ cell tumors as types I, II or III during tumor progression in each patient. We based classification primarily on tumor size and the presence of cystic components by the consensus of two radiologists (I.O.K and S.M.L, with 35 and 6 years of experience, respectively). The classification criteria were as follows: type I, ill-defined patchy lesions (<3 cm) without cystic components, mainly visible on T2-weighted images; type II, small mass lesions (<3 cm) with a cystic component; and type III, large lesions (≥3 cm) with cystic components (Fig. 1). Tumor areas were considered cystic when they were isointense compared with cerebrospinal fluid on T2-weighted images and isointense to hypointense compared with brain parenchyma on T1-weighted images.

We grouped the 15 basal ganglia germ cell tumors according to a change in tumor type between initial MRI and diagnostic MRI (the study at the time of diagnosis), analyzing the following findings: (1) time interval between the onset of symptoms and initial MRI (symptom duration), (2) time interval between initial MRI and diagnostic MRI (MRI nearest the time of diagnosis), and (3) alteration of MRI features between initial MRI and diagnostic MRI. We examined the following features: tumor size, cyst size, the size ratio of the cystic component to the tumor (cyst/mass), the presence of intratumoral hemorrhage, associated ipsilateral cerebral hemispheric or brainstem hemiatrophy, and enhancement patterns. Tumor and cyst size were based on the largest diameter measured on axial T2-weighted images. In calculating cyst/mass ratio, we defined cyst size as the largest diameter of the conglomerate cystic portion. Intratumoral hemorrhage was indicated by any one of the following criteria: (1) hyperintensity on T1-weighted images and hyperintensity or marked hypointensity on T2-weighted images, (2) a fluid-fluid level with marked hypointensity in the dependent portion on T2-weighted images, and (3) an intratumoral cyst with a markedly hypointense rim on T2-weighted images/susceptibility-weighted images/T2* gradient-echo images or marked hypointensity of intratumoral cyst on
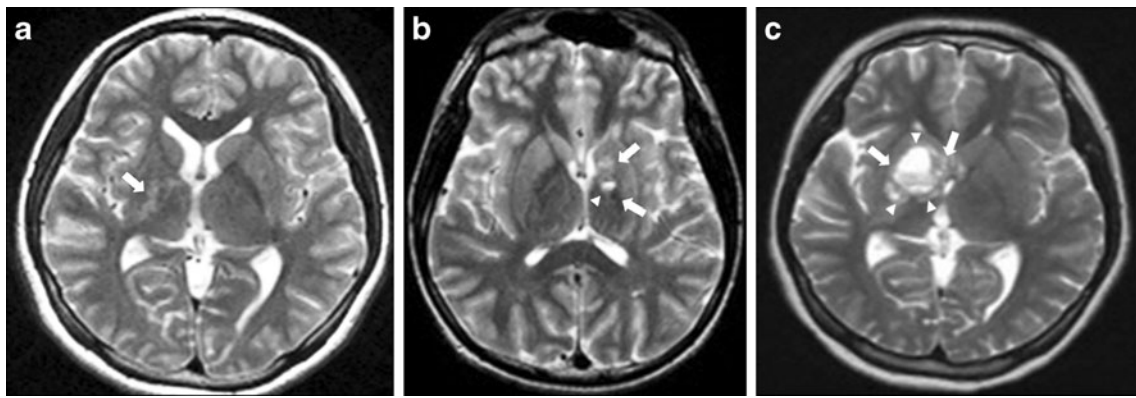
Fig. 1 Brain MRI tumor classification. **a** Axial T2-weighted turbo spin-echo MRI (TR/TE=5000/121 ms) in a 10-year-old boy with germinoma type I tumor shows ill-defined patchy lesions (<3 cm) without cystic components (*arrow*). **b** Axial T2-weighted turbo spin-echo MRI (TR/TE=5000/99 ms) in a 16-year-old boy with germinoma type II tumor shows small mass lesions (<3 cm) (*arrows*) with a cystic component (*arrowhead*). **c** Axial T2-weighted turbo spin-echo MRI (TR/TE=5000/96 ms) in an 18-year-old man with germinoma type III shows a large lesion (≥3 cm) (*arrows*) with cystic components (*arrowheads*)

susceptibility-weighted images/T2*-weighted gradient-echo images.

Results

Changes in tumor type, duration of symptoms, and time interval between initial MRI and diagnostic MRI are summarized in Table 1. In initial MRI examinations, 11 of 15 germ cell tumors were classified as type I, and 4 as type II. During the follow-up period, 8 type I tumors progressed to types II or III, and 3 type II tumors progressed to type III. One tumor underwent a staged change from type I to type III in two steps (Fig. 2). Four of the 15 tumors did not change in type during the follow-up period. The duration of symptoms and time intervals between initial MRI and definitive diagnosis were variable. Time interval between type changes was variable in each tumor. Mean time between type changes was 3.5 months for types I to II, 17 months for types I to III, and 7.6 months for types II to III (Table 1).

At initial MRI examination, 13 tumors showed patchy signal abnormalities with irregular margins and the remaining 2 showed relatively well-marginated mass lesions. The centers of the tumors appeared as lentiform nuclei in 12, the head or body of the caudate nucleus in 2, and a diffuse expansile basal ganglia lesion in 1. Two of 15 tumors were restricted to the basal ganglia and that remained unchanged during the follow-up period. The remaining 13 tumors extended into the internal capsule on initial MR images; six of them involved additional structures including the periphery of the thalamus ($n=4$) and deep white matter adjacent to the basal ganglia ($n=2$). As these tumors grew, 4 of the 13 extended farther into the thalamus, adjacent white matter and midbrain.

Alterations in MRI features during tumor progression are listed in Table 2. During progression, all but three (type I to I in two, and types I to II in one) increased in size. Tiny cystic components (size range 4–5 mm) developed in all five tumors that changed from types I to II (Fig. 3); however overall size of most of the tumors (4/5, 80%) did not change or minimally increased (range 2–4 mm). In addition, the tumor that had undergone a staged change from type I to type III in two steps

Table 1 Interval changes in tumor type from initial MRI to MRI at time of diagnosis

Change of the tumor type from initial MRI to MRI at time of diagnosis [a]	Tumor ($n=15$)	Symptom duration[b] (months)	Interval from initial MRI to MRI at time of diagnosis[b] (months)
I→I	3 (20%)	2.3 (0–5)	15.7 (2.4–33.1)
I→II	5 (33%)	2 (0–3)	3.5 (2.2–7.2)
I→III	3 (20%)	2.7 (0.2–4)	17 (9.8–30.6)
II→II	1 (7%)	10	15.5
II→III	3 (20%)	5 (1–12)	7.6 (1.5–19)

[a] The classification criteria of tumor type were as follows: type I, ill-defined patchy lesions (<3 cm) without cystic components, mainly visible on T2-weighted images; type II, small mass lesions (<3 cm) with a cystic component; and type III, large lesions (≥3 cm) with cystic components

[b] Data show mean values, with ranges in parentheses
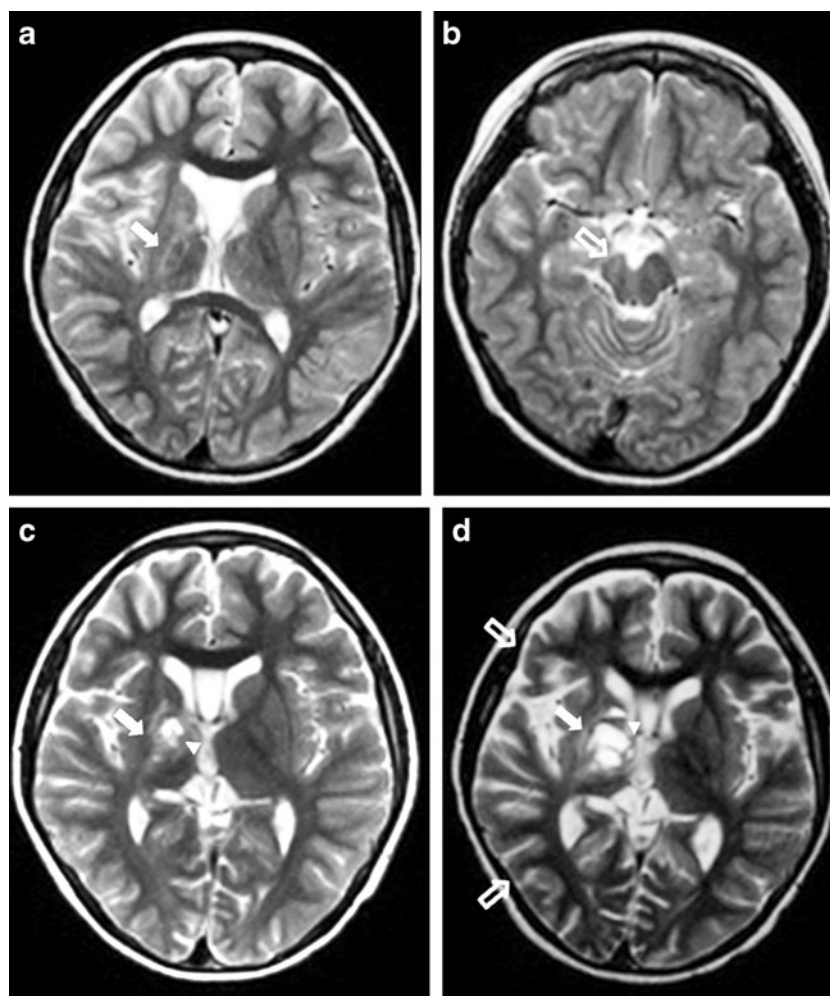
Fig. 2 Brain MRI in a 10-year-old boy with germinoma in the right basal ganglia. All MR images obtained from other hospitals before admission. MR images (**a** and **b**) was performed due to slowly progressive left hemiparesis for 4 months. **a–d** Axial T2-weighted turbo spin-echo images (TR/TE = 3,500/104 ms) illustrate a staged change from type I to type III in two steps: (**a, b**) type I tumor, (**c**) type II tumor, (**d**) type III tumor. **a** Initial MRI shows tumor as an ill-defined hyperintense lesion without a cystic component or mass effect in the right lentiform nucleus and internal capsule (*arrow*). **b** Initial MRI shows atrophic change in the brainstem (*arrow*). **c** Five months after initial MRI, tumor (*arrow*) shows cystic change (*arrowhead*) and increased size. **d** Eleven months after initial MRI, tumor has changed to an overt large mass (*solid arrow*) with multiple cysts of various sizes. T2-weighted image shows cysts with fluid-fluid levels that are hypointense in the dependent portion, considered to be an intracystic hemorrhage (*arrowhead*). Ipsilateral hemiatrophy (atrophy of ipsilateral basal ganglia, cortical atrophy, and brainstem atrophy) is more pronounced with tumor progression (*open arrows*). *TE* echo time, *TR* repetition time

developed a small cyst (5 mm) 5 months after initial MRI; this tumor also increased in size from 16 mm to 22 mm during that time and was therefore re-classified as type II. (11 months after initial MRI), this tumor had progressed to an overt large mass with multiple cysts and was classified as type III. Generally as tumors grew, the size of the cystic component in the solid mass increased, and multiple cysts of various sizes could be observed. The cyst/mass ratio also increased during tumor progression.

As tumors progressed, intratumoral hemorrhage became more common and obvious. Hemorrhage was observed in all type III tumors (6/6, 100%) and most type II tumors (6/9, 67%) on conventional MR images. Various hemorrhage patterns coexisted within a single tumor, although hemorrhage

was not confirmed histologically. MRI of types II and III tumors indicated the following: hematomas in 2 lesions (1 type II, 1 type III), fluid-fluid levels with marked hypointensity in the dependent portion on T2-weighted images in 8 lesions (5 type II, 3 type III), presumed old hemorrhagic cysts in 11 lesions (5 type II, 6 type III). Three of 4 type I tumors (75%) that were evaluated using susceptibility/T2*-weighted gradient-echo imaging had hypointense foci that were hardly detectable on conventional images (Fig. 4).

Ipsilateral hemispheric and brainstem atrophy was observed in most type I tumors (9/11, 82%) and all four type II tumors on initial MR images. Two type I tumors that did not show obvious hemiatrophy were confined to the basal ganglia

Table 2 Interval changes in tumor type and MRI features from initial MRI to MRI at the time of diagnosis

Change of the tumor type[a] (n = 15)	Mass size[b] (mm)		Cyst size[b] (mm)		Cyst/mass[b] (%)		Hemorrhage[c]		Enhance[c]	
	Initial	Diagnostic	Initial	Diagnostic	Initial	Diagnostic	Initial	Diagnostic	Initial	Diagnostic
I→I (n=3)	14.9 (10–21.6)	16.7 (10–27)	-	-	-	-	0	0	2	2
I→II (n=5)	18.4 (11–23)	22.4 (18–26)	-	4.4 (3.5–5.4)	-	24.6 (16.7–42)	0	2	2	4
I→III (n=3)	14.2 (9.7–17)	39.7 (31–56)	-	25.9 (22.7–29)	-	77.9 (59–93.5)	0	3	0	3
II→II (n=1)	25	28	10	13.2	40	47.1	1	1[d]	1	1
II→III (n=3)	23.3 (22–25)	35 (31–39)	6.3 (5.2–7.3)	18.1 (8.9–32.5)	34.6 (24–52)	57.8 (37.9–83.3)	3	3[d]	3	3

Initial Initial MRI, *Diagnostic* MRI at the time of diagnosis

[a] The classification criteria of tumor type were as follows: type I, ill-defined patchy lesions (<3 cm) without cystic components, mainly visible on T2-weighted images; type II, small mass lesions (<3 cm) with a cystic component; and type III, large lesions (≥3 cm) with cystic components

[b] Data show mean values, with ranges in parentheses

[c] Data show the number of tumors with internal hemorrhage or enhancement on conventional MR images

[d] More pronounced in the follow-up study

without evident involvement of the internal capsule; one appeared as an expansile lesion involving the basal ganglia, and the other was localized in the lentiform nucleus (Fig. 4). In contrast, tumors with ipsilateral hemiatrophy involved the

Fig. 3 Brain MRI in an 11-year-old boy with mixed germ cell tumor in the left basal ganglia. **a** Axial T2-weighted turbo spin-echo image (TR/TE = 9,000/103 ms) shows an ill-defined hyperintense lesion in the left lentiform nucleus and internal capsule (type I) (*solid arrow*). Ipsilateral hemiatrophy can be seen in the basal ganglia (*open arrows*). **b** Axial T2-weighted turbo spin-echo image (TR/TE = 4,000/107 ms) obtained 2 months after initial MRI shows tiny cysts with fluid-fluid level of hyperintensity and marked hypointensity (*arrowhead*) within the tumor (type II) (*arrow*).. **c, d** MR images obtained 6.5 months after initial MR images. **c** Axial T2-weighted turbo spin-echo image (TR/TE = 4,000/107 ms) shows an increase in size of cystic components as well as the whole tumor (*arrow*). The tumor is less than 3 cm and is therefore classified as type II. **d** Unenhanced axial T1-weighted turbo spin-echo image (TR/TE = 570/10 ms) shows hyperintensity within cysts (*arrowheads*), which suggests intracystic hemorrhage. *TE* echo time, *TR* repetition time
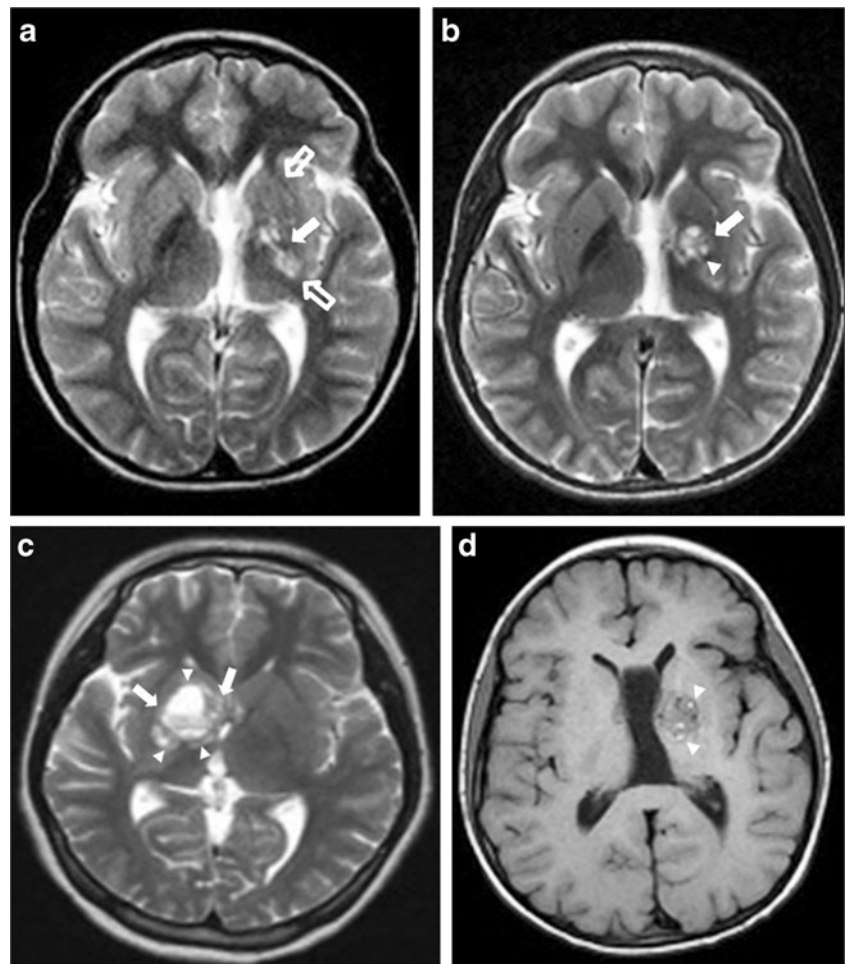
Fig. 4 Brain MRI in a 7-year-old boy with germinoma that was unchanged in type (type I). **a** Axial T2-weighted turbo spin-echo image (TR/TE = 3,000/80 ms) shows an ill-defined patchy hyperintense lesion, relatively confined to the right lentiform nucleus (*arrow*). **b** Axial T2*-weighted gradient echo image (TR/TE = 537/12 ms) shows hypointense foci in the mass lesion, indicating microhemorrhage (*arrow*). **c** Axial T2-weighted turbo spin-echo image (TR/TE = 3,000/80 ms) shows no obvious atrophy in the brainstem (*arrow*) but shows asymmetrical frontal horn of lateral ventricle. **d** Axial T2-weighted turbo spin-echo image (TR/TE = 6,600/136 ms) obtained 2 months after initial MR images shows slight progression of the ipsilateral hemiatrophy at the cerebral hemisphere (*open arrows*), although tumor (*solid arrow*) size is not changed and internal capsule involvement of the tumor is not evident. *TE* echo time, *TR* repetition time
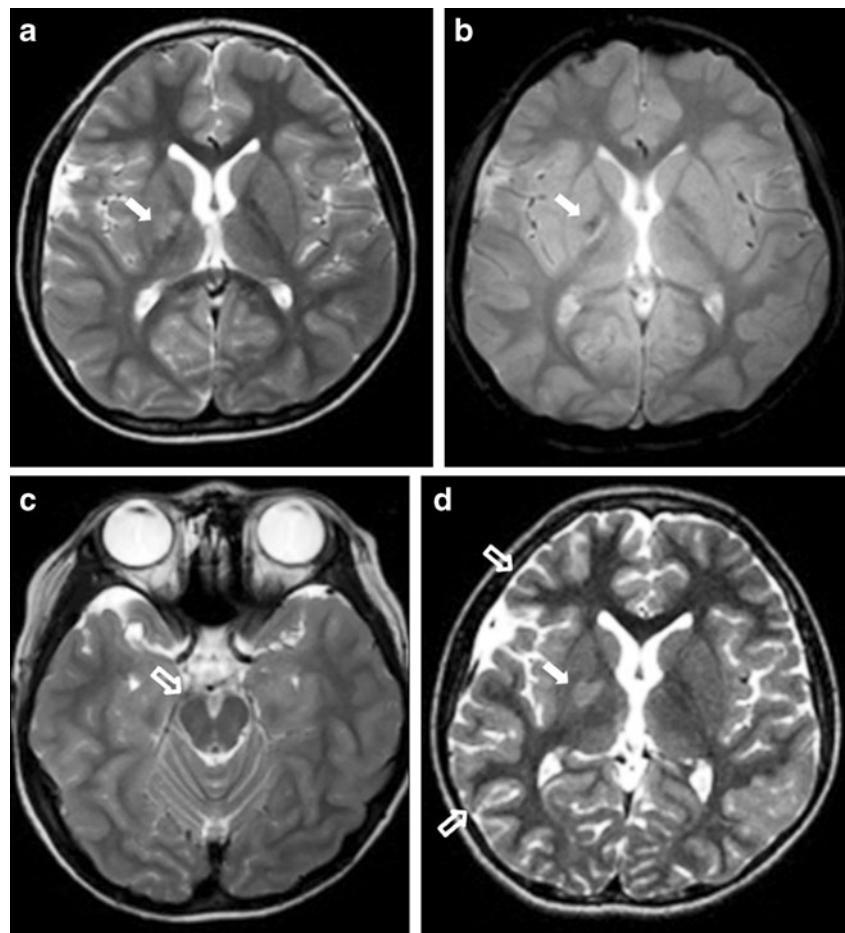
internal capsule or the periphery of the thalamus, showing irregular margins. Ipsilateral hemiatrophy was more pronounced during tumor progression in all cases; the two tumors without obvious hemiatrophy on initial MR images (type I to I in one, type I to II in one) showed atrophic changes after 2 months and 3 months, although size change was minimal (0 mm and 2 mm) and internal capsule involvement was not evident.

Tumor enhancement was seen in 36% of type I (4/11), 89% of the type II (8/9) and 100% of type 3 tumors (Table 2). As tumors progressed, the enhancement became more prominent and heterogeneous; enhancement was marked in all type III tumors and two type II tumors, mild in six type II tumors, and faint in four type I tumors.

The four basal ganglia germ cell tumors in the study that showed no change in type during the follow-up period did, however, show evident progression on follow-up MR images. Overall tumor size increased in two tumors (type I to I in one, type II to II in one) and cyst size and cyst/mass ratio also increased in one tumor (type II to II). Ipsilateral hemiatrophy was more obvious during the follow-up period in these four tumors, including the two tumors that did not change in size.

Discussion

We classified basal ganglia germ cell tumors into three distinct types based on MR findings. Analysis of serial MR images showed sequential progression from type I to type III. Ill-defined small hyperintense lesions without cystic components as seen on T2-weighted images progressed to larger masses with cystic components, and ultimately to overt large masses with multiple cysts of various sizes.

Several reports have shown the presence of cysts in basal ganglia germ cell tumors at frequencies ranging 50–100% [5, 7, 9, 10, 23]. Although multiple intratumoral cysts of various sizes are typically found in late-stage basal ganglia germ cell tumors [3, 7, 9, 10], our study revealed that intratumoral cysts can occur at a relatively early stage during progression. In our study, all type II tumors that had changed from type I had a few small cysts (3.5–5.4 mm), whereas overall size of these tumors (4/5, 80%) did not change or only minimally increased (range 0–4 mm) during tumor progression. The time interval between the changes was a mean 3.5 months (range 2.2–7.2 months). Tumor presenting as a small basal ganglia mass lesion containing a few tiny cysts at initial MRI, which was classified as type II tumor in our study, can be mistaken for a

nontumorous condition such as vasculitis, cavernous malformation or cerebral infarction.

Cysts reportedly result from either necrosis or repeated intratumoral hemorrhage [5, 7, 10] and often contain xanthochromic fluid, which suggests old hemorrhage. In our study, many cysts had fluid-fluid levels with marked hypointense dependent layering or dark-intensity rims on T2-weighted images, and this was the most common pattern of the intratumoral hemorrhage. Although hemorrhage was not confirmed histologically, these findings are consistent with intracystic hemorrhage. Tumor enlargement can be accounted for with cyst formation and intratumoral hemorrhage [9, 10]. Several reports have shown that cyst formation and hemorrhage correlate with tumor size [9–11]. In the study by Kim et al. [9], 12 germ cell tumors larger than 20 mm in diameter had conspicuous cysts (while 2 smaller germ cell tumors did not) and 7 of the 12 had intratumoral hemorrhage. Similarly, in our study all but one of the types II and III germ cell tumors had cystic components and were larger than 20 mm in diameter, while 64% (7/11) of type I tumors (without a cystic component) were smaller than 20 mm. Moreover, as tumors grew the cysts not only increased in size but also occupied a greater portion of the tumor. Intratumoral hemorrhage also became more pronounced as tumors grew. In our study intratumoral hemorrhage was observed in all type III and most type II tumors (6/9, 67%), while no type I tumors showed intratumoral hemorrhage on conventional MR images. However, 3 of 4 type I tumors examined via susceptibility/T2*-weighted gradient-echo imaging did show hypointense foci that did not correspond to calcification on CT; those hypointense foci were presumed to represent microhemorrhage. Therefore, even type I germ cell tumors, which are considered to be early stage tumors, may contain hemorrhagic content. Because the remainder of type I tumors were not examined via this imaging method, the presence of microhemorrhage might be underestimated in our study. Lou et al. [11, 12] showed that early stage basal ganglia germinomas, defined as small (<10 mm) patchy hyperintense lesions on T2-weighted images without cystic components, appeared as obvious hypointense lesions on susceptibility-weighted images as a result of intratumoral hemorrhage.

Ipsilateral hemiatrophy, which occurs at a frequency of 17–100%, might also be useful for diagnosing basal ganglia germ cell tumors [5–7, 9, 13]. In our study, ipsilateral hemiatrophy was seen in 87% (13/15) of germ cell tumors on initial MR images. Differences in frequency could be associated with tumor size. Ozelame et al. [13] and Okamoto et al. [6] reported that all germ cell tumors examined in their studies, in which the tumors were generally small and in the early stages, showed ipsilateral hemiatrophy on initial neuroimages. In contrast, studies showing low frequencies of ipsilateral hemiatrophy in germ cell tumors (17% and 21%) included mostly large tumors [5, 9]. In our study, three tumors

(two type I, one type II) showed atrophic change in the brainstem and basal ganglia on initial MR images, but cortical atrophy was not evident. As tumors progressed to type III, previously noted mild atrophy in the basal ganglia was masked by extensive tumor involvement, and atrophic change was detected only in the brainstem. Therefore hemiatrophy can be overlooked with tumor growth if coexisting brainstem or cortical atrophy is not remarkable. Ipsilateral hemiatrophy could result from Wallerian degeneration caused by tumor infiltration of fiber tracts [24, 25]; therefore it may be related with tumor location. In our initial MR images, tumors that were associated with ipsilateral hemiatrophy involved the internal capsule. Tumors restricted to the basal ganglia showed only subtle enlargement of the anterior horn of the ipsilateral lateral ventricle, without definite hemiatrophy. Ipsilateral hemiatrophy may be also related to the growth rate of tumors [15, 26]. Mutoh et al. [26] proposed that slowly growing tumors could develop ipsilateral hemiatrophy. These authors found that astrocytomas involving frontal or occipital lobes and basal ganglia germinomas showed similar atrophic change [26]. In our study two tumors without obvious hemiatrophy on initial MR images showed mild cerebral and brainstem hemiatrophy on follow-up MR images performed after 2 months and 3 months, respectively, although tumor involvement of the internal capsule was not seen.

Our study had several limitations. First, MRI protocols, parameters and follow-up intervals were not standardized because some MRI data were obtained from other hospitals before the patient entered our hospital. Second, cystic changes and intratumoral hemorrhage were not histologically confirmed. Therefore, other factors, most notably calcification, might have been misinterpreted as microhemorrhage; however, this discrimination could be made on CT images.

Conclusion

Early stage basal ganglia germ cell tumors appear as ill-defined small hyperintense lesions without cystic components on T2-weighted images, are almost always associated with ipsilateral hemiatrophy, and sometimes display microhemorrhage. Tumors develop tiny cysts at a relatively early stage, and therefore basal ganglia germ cell tumors should be considered as one of the differential diagnoses when, added to the aforementioned findings, few tiny cysts are observed in the basal ganglia, especially in boys.

References

1. Packer RJ, Cohen BH, Cooney K (2000) Intracranial germ cell tumors. Oncologist 5:312–320

2. Echevarria ME, Fangusaro J, Goldman S (2008) Pediatric central nervous system germ cell tumors: a review. Oncologist 13:690–699

3. Raybaud C, Barkovich AJ et al (2012) Intracranial, orbital, and neck masses of childhood. In: Barkovich AJ, Raybaud C (eds) Pediatric neuroimaging. Lippincott Williams & Wilkins, Philadelphia

4. Crawford JR, Santi MR, Vezina G et al (2007) CNS germ cell tumor (CNSGCT) of childhood: presentation and delayed diagnosis. Neurology 68:1668–1673

5. Soejima T, Takeshita I, Yamamoto H et al (1987) Computed tomography of germinomas in basal ganglia and thalamus. Neuroradiology 29:366–370

6. Okamoto K, Ito J, Ishikawa K et al (2002) Atrophy of the basal ganglia as the initial diagnostic sign of germinoma in the basal ganglia. Neuroradiology 44:389–394

7. Higano S, Takahashi S, Ishii K et al (1994) Germinoma originating in the basal ganglia and thalamus: MR and CT evaluation. AJNR Am J Neuroradiol 15:1435–1441

8. Rasalkar DD, Chu WC, Cheng FW et al (2010) Atypical location of germinoma in basal ganglia in adolescents: radiological features and treatment outcomes. Br J Radiol 83:261–267

9. Kim DI, Yoon PH, Ryu YH et al (1998) MRI of germinomas arising from the basal ganglia and thalamus. Neuroradiology 40:507–511

10. Moon WK, Chang KH, Kim IO et al (1994) Germinomas of the basal ganglia and thalamus: MR findings and a comparison between MR and CT. AJR Am J Roentgenol 162:1413–1417

11. Lou X, Ma L, Wang FL et al (2009) Susceptibility-weighted imaging in the diagnosis of early basal ganglia germinoma. AJNR Am J Neuroradiol 30:1694–1699

12. Lou X, Tian C, Chen Z et al (2012) Differential diagnosis of infarct-like intracranial ectopic germinomas and subacute lacunar infarct on susceptibility-weighted imaging. J Magn Reson Imaging 36:92–98

13. Ozelame RV, Shroff M, Wood B et al (2006) Basal ganglia germinoma in children with associated ipsilateral cerebral and brain stem hemiatrophy. Pediatr Radiol 36:325–330

14. Phi JH, Cho BK, Kim SK et al (2010) Germinomas in the basal ganglia: magnetic resonance imaging classification and the prognosis. J Neurooncol 99:227–236

15. Wong ST, Yuen SC, Fong D (2009) Pathophysiological mechanism of ipsilateral cerebral and brainstem hemiatrophy in basal ganglia germ cell tumors: case report. Childs Nerv Syst 25:693–699

16. Fujii Y, Saito Y, Ogawa T et al (2008) Basal ganglia germinoma: diagnostic value of MR spectroscopy and (11)C-methionine positron emission tomography. J Neurol Sci 270:189–193

17. Lee J, Lee BL, Yoo KH et al (2009) Atypical basal ganglia germinoma presenting as cerebral hemiatrophy: diagnosis and follow-up with 11C-methionine positron emission tomography. Childs Nerv Syst 25:29–37

18. Sudo A, Shiga T, Okajima M et al (2003) High uptake on 11C-methionine positron emission tomographic scan of basal ganglia germinoma with cerebral hemiatrophy. AJNR Am J Neuroradiol 24:1909–1911

19. Jager PL, Vaalburg W, Pruim J et al (2001) Radiolabeled amino acids: basic aspects and clinical applications in oncology. J Nucl Med 42:432–445

20. Nakagawa M, Kuwabara Y, Sasaki M et al (2002) 11C-methionine uptake in cerebrovascular disease: a comparison with 18F-fDG PET and 99mTc-HMPAO SPECT. Ann Nucl Med 16:207–211

21. Coakley J, Kellie SJ, Nath C et al (2005) Interpretation of alpha-fetoprotein concentrations in cerebrospinal fluid of infants. Ann Clin Biochem 42:24–29

22. Fujimaki T, Mishima K, Asai A et al (2000) Levels of beta-human chorionic gonadotropin in cerebrospinal fluid of patients with malignant germ cell tumor can be used to detect early recurrence and monitor the response to treatment. Jpn J Clin Oncol 30:291–294

23. Tang J, Ma Z, Luo S et al (2008) The germinomas arising from the basal ganglia and thalamus. Childs Nerv Syst 24:303–306

24. Kwak R, Suzuki J (1970) Brain tumor with ipsilateral cerebral hemiatrophy. No To Shinkei 22:1439–1446

25. Kuhn MJ, Johnson KA, Davis KR (1988) Wallerian degeneration: evaluation with MR imaging. Radiology 168:199–202

26. Mutoh K, Okuno T, Ito M et al (1988) Ipsilateral atrophy in children with hemispheric cerebral tumors: CT findings. J Comput Assist Tomogr 12:740–743